Fermi National Accelerator Laboratory

Final Report

Moνving Knowledge 2017

Fermilab - CAIF 2017

Cosmic Ray Studies for SBND

Submitted By:
Michele Piero Blago

Supervised By:
Prof. Roxanne Guenette
Dr. Corey Adams

Contents

Abstract

The Short-Baseline Near Detector (SBND) is one of three Liquid Argon Detectors using the Booster Neutrino Beam at Fermilab with the goal to search for sterile neutrinos and to refine the neutrino-argon cross-section. The experiment is currently in the construction phase and planned to start operation in 2019. The detector is located close to the surface and hence subject to a large cosmic ray induced background. This makes a precise simulation of the detector geometry and facilities crucial to investigate the influence of cosmic ray particles.
The study carried out by the author validates the detector geometry simulation and cosmic particle generation. The preliminary data sets are used to compare the effect of an overburden with 1 m thickness to a scenario without overburden. A series of background reduction cuts are investigated to reduce the single photon background.

1 Introduction

The Short-Baseline Neutrino (SBN) Program at Fermilab has the objective to perform the to date most sensitive search for sterile neutrinos at the eV mass-scale. Evidence for the existence of sterile neutrinos can be provided through standard model neutrino appearance and disappearance channels. The second major objective of the SBN Program is to provide a precise measurement of the neutrino-argon cross-section. This is particularly relevant for future large-scale liquid argon experiments, such as the DUNE detector.

1.1 SBN Experiments

The SBN Program consists of three detectors, positioned at varying distances along Fermilab's Booster Neutrino Beam (BNB), as shown in Figure 1. This allows to sample the neutrino spectrum as a function of distance. All three detectors are Liquid Argon Time Projection Chambers (LAr-TPCs). The SBN far detector, ICARUS, is positioned at 600 m distance to the BNB target. It is the largest of the three

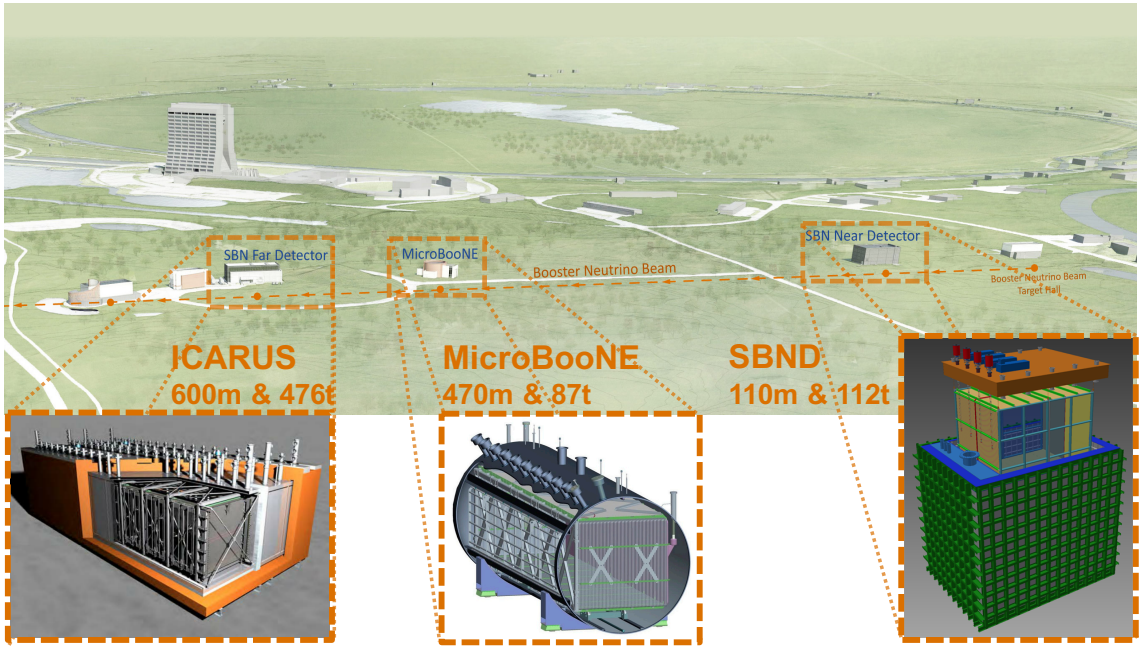

Figure 1: The three liquid argon detectors of the SBN Program along with the Booster Neutrino Beam. ICARUS (left) at a distance of 600 m to the BNB target with an active volume of 476 t, MicroBooNE at 470 m and with 87 t, and SBND at 110 m and with and active volume of 112 t. Adapted from [7].

detectors with an active detector volume of 476 t and is currently in the construction phase. MicroBooNE is responsible for measuring neutrino oscillations at the intermediate distance of 470 m [1]. It has an active volume of 87 t and is taking data since 2015 [4]. The Short-Baseline Near Detector (SBND) is the detector located closest to the target at a distance of 110 m which measures the unoscillated neutrino spectrum in an active volume of 112 t. It is in the construction phase with a planned start of operation in 2019.

The three SBN detectors are surface detectors and hence subject to cosmic radiation which imposes a large background that can mimic the experiment's signal. This study focuses on the impact of cosmic radiation on SBND. In particular, the expected amount of particles and their energies is determined. Comparisons to results published by MicroBooNE are made.

1.2 Short-Baseline Neutrino Detector

The SBND consists of two time projection chambers with 2 m drift distance each [1]. At 500 V/cm the maximum drift time is 1.28 ms. When a charged particle enters the cryostat it ionises the liquid argon along its track. The resulting electrons drift along the electric field to three wire planes. The wire planes are separated by a 3 mm pitch and are oriented at 0° and ±60° with respect to the vertical. The three wire planes allow a spatial resolution of the track. The scintillation light produced by the traversing particle is collected by 120 8 inch photomultiplier tubes. This provides an immediate time stamp of the corresponding track. Figure 2 shows a schematic of the two SBND TPCs. The coordinate system is also depicted. The origin of the coordinate system is defined as the centre of the upstream TPC wall. The Z-axis corresponds to the beamline. Additionally, the cryostat is surrounded by 7 cosmic

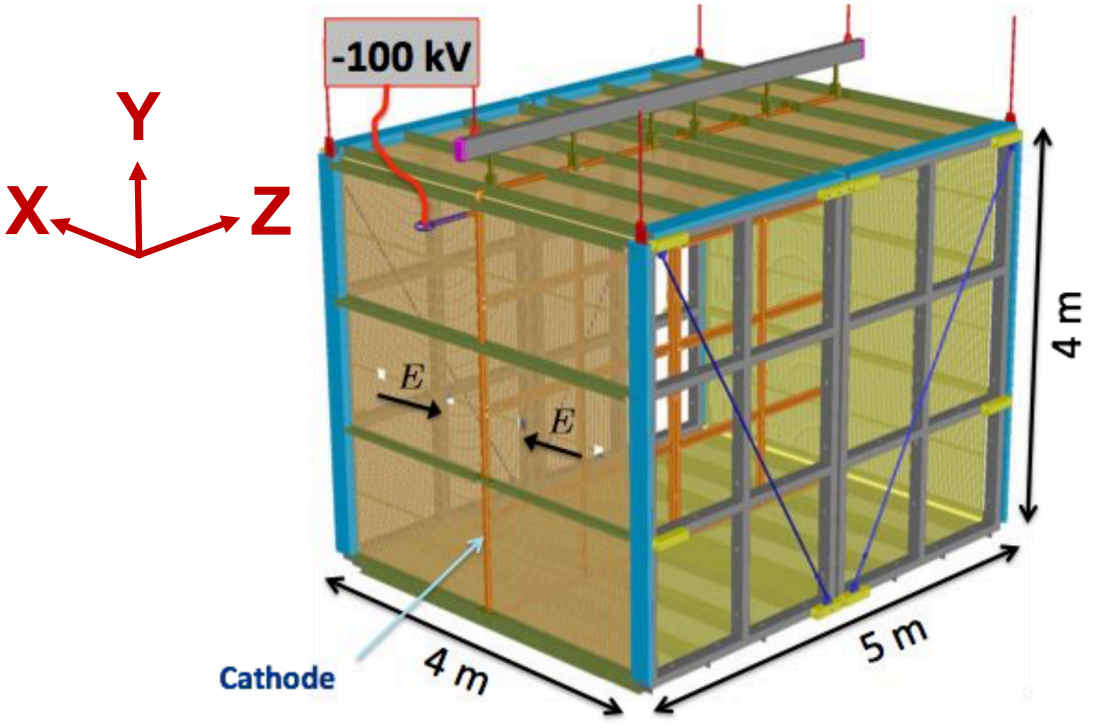

Figure 2: Schematic of the SBND with coordinate system.

ray detection planes. Two of these Cosmic Ray Taggers (CRTs) are located above the cryostat to provide a track measurement of cosmic particles which enter and

stop inside the TPC. The CRT system is an essential feature of the SBND due to its location on close to the surface. The main objective of the CRTs is to track cosmic muons which are likely to produce a background in the TPC.

2 Detector simulation

To reproduce the SBND experiment the detector as well the major structural features in the surrounding are simulated. For this purpose GDML [3] is used for geometry and material description. Figure 3 shows the GDML visualisation of the detector geometry and its surrounding structure. The simulation contains the detector building, the cryostat, the time projection chamber, and the cosmic ray taggers. A concrete overburden (OB) of 1 m thickness can be activated. Cosmic ray particles

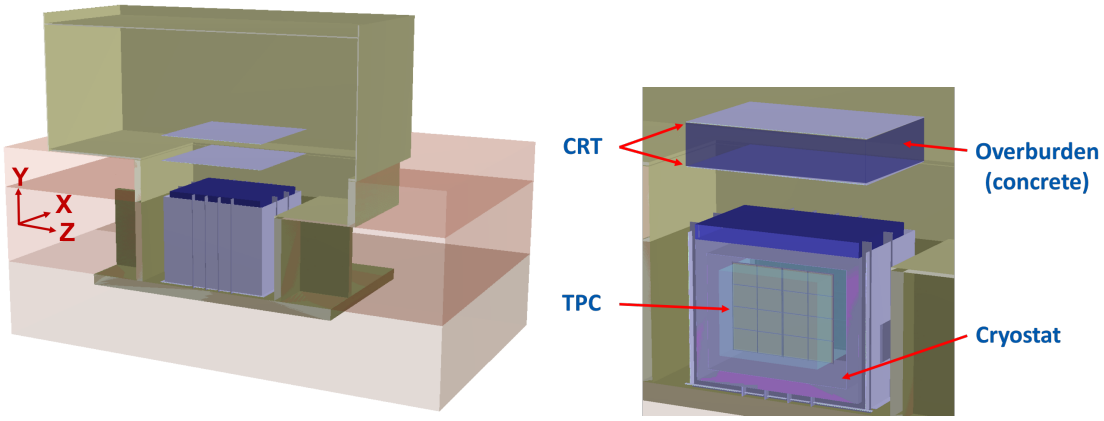

(a) (b)

Figure 3: The SBND detector and building geometry simulation, generated with GDML. Structural components of the building are shown in green, the liquid argon cryostat in dark blue and the cosmic ray detection planes in light blue. (b) shows a vertical cut of (a) which makes the TPC visible and the photocathode located in its centre. A concrete overburden can be activated in the simulation between the two top CRT planes.

are produced using the CORSIKA CMC FLUKA [6] simulation program. CORSIKA was chosen since it allows more accurate tuning of parameters than other cosmic ray generators as for example CRY [5], which was previously used. The Constant Mass

Composition (CMC) model serves the purpose of generating primary particles in a large variety. FLUKA describes the flux modeling and is well equipped for hadron interactions at low energies, which are most relevant to the experiment. A detailed comparison of the generators can be found in [4].
The generated particles traverse the detector and building geometry using the GEANT4 high-energy simulation toolkit [2] to propagate the particles according to the appropriate physical interactions and decays.
The entire simulation structure, including the detector geometry and cosmic particle generation as well as their propagation through the components, will be referred to in this text as simulation.

2.1 Geometry validity check

The detector geometry and cosmic particles which are generated as explained above were cross-checked in this study. This represents an integral part of determining the validity of the simulation construct. Particle start and end point positions were investigated. This allows to visualise the active volume components of the simulation. At the same time, it provides a qualitative indication of high particle interaction activity, as is expected from the liquid argon in the cryostat, but may also occur for other components of high density. Figure 4 shows the particle end point distribution from a downstream and from a side perspective. The TPC is illustrated as a black box in the histogram. The cryostat is clearly visible due to a large amount of particles stopping in the liquid argon.

3 Simulated cosmogenic background

The cosmogenic background is studied. The number of particles in the TPC is determined and normalised to 1.5 ms, corresponding to the SBND read-out window. Two samples are compared, in one of the samples the concrete overburden is present to study its impact. Figure 5 shows the same picture as in Figure 4 but with the OB in place. In these histograms, the downstream area of the cryostat features

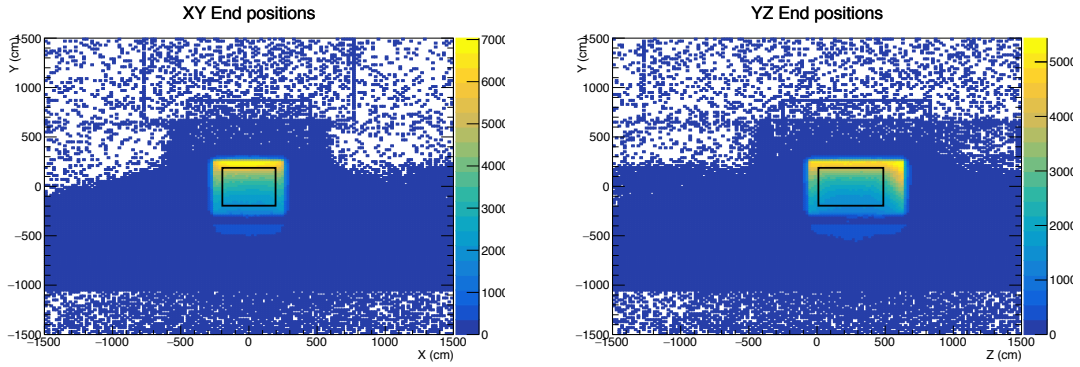

(a) (b)

Figure 4: Downstream view of the particle end positions in the simulation without overburden (a). (b) shows the side perspective of the particle end positions in the simulation. In both figures, the position of the TPC is illustrated as a black box.

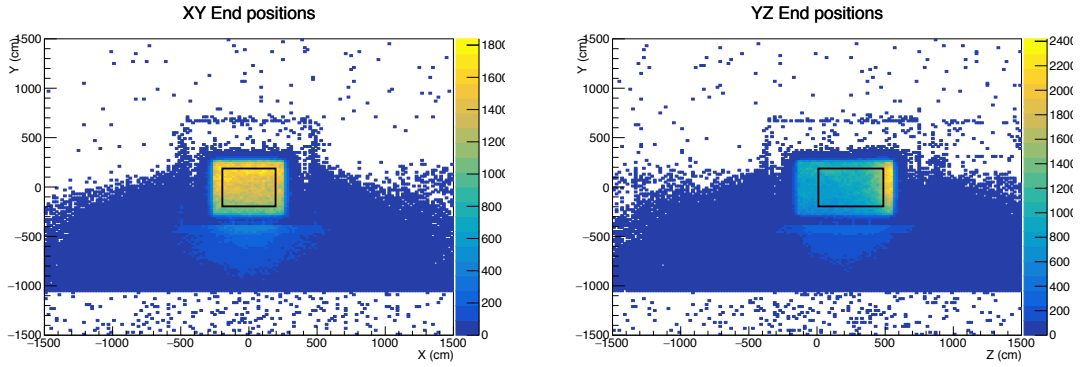

(a) (b)

Figure 5: Downstream view of the particle end positions in the simulation with overburden (a). (b) shows the side perspective of the particle end positions in the simulation. In both figures, the position of the TPC is illustrated as a black box. A high activity is visible at the downstream side of the TPC due less shielding from the building structure.

a significantly higher amount of stopping particles. This is a result of the lack of structural shielding on the downstream side of the detector, as illustrated in Figure 6.

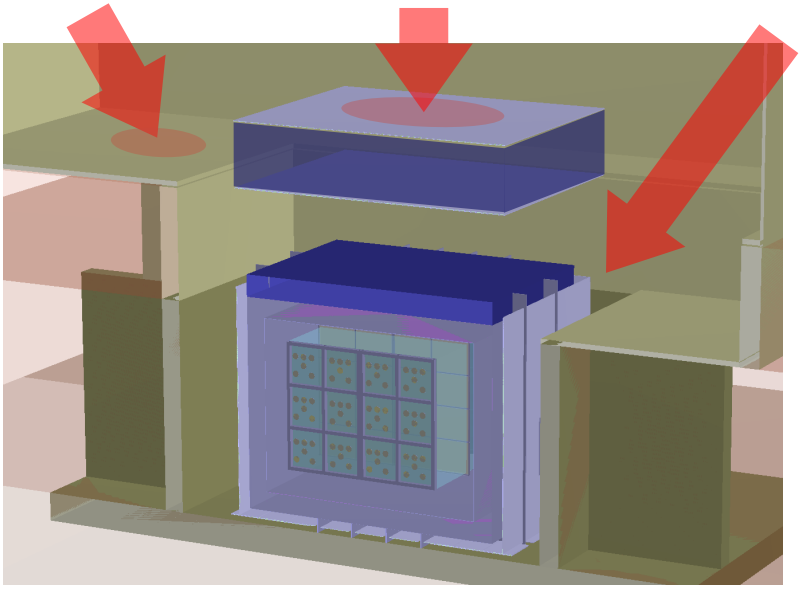

Figure 6: Simulation picture of the detector and building geometry. Red arrows illustrate cosmic radiation, which is reduced by the overburden and the building structure on the upstream side. The downstream side, where the access to the detector is located, represents a leak for cosmic particles.

3.1 Cosmogenic particle rates and energies

The rates for particles entering the TPC active volume normalised to 1.5 ns are presented in Table 1 and 2 for the detector without and with OB, respectively. Particles of interest are muons and antimuons, neutrons and protons, electrons and positrons, and photons. For electrons and protons, an energy cut at 100 MeV is applied to remove particles below this energy which are not relevant in the context of this study.

For both cases, with and without overburden, no primary electrons and only a negligible amount of primary photons reach the detector. They are most likely absorbed by the material surrounding the detector. Secondary electrons and photons are present in the active volume of the detector. The starting point distribution of secondary photons which enter the TPC is shown in Figure 7. One can see that most secondary photons which enter the detector are created either inside the liquid argon of the TPC or by the walls of the cryostat.

Particle Type	Primaries	CORSIKA CMC FLUKA Secondaries	Total
μ^-	10.406 ± 0.007	0.00030 ± 0.00001	10.406 ± 0.007
μ^+	12.977 ± 0.007	0.0024 ± 0.0001	12.979 ± 0.007
neutron	0.0988 ± 0.0006	0.647 ± 0.002	0.736 ± 0.002
proton	0.0013 ± 0.0001	0.373 ± 0.001	0.374 ± 0.001
γ (>100 MeV)	0.0001 ± 0.00001	0.0039 ± 0.0001	0.0040 ± 0.0001
e^- (>100 MeV)	0.0 ± 0.0	0.0020 ± 0.0001	0.0020 ± 0.0001
e^+ (>100 MeV)	0.0 ± 0.0	0.0024 ± 0.0001	0.0024 ± 0.0001

Table 1: The particle rates expected in the detector without overburden, normalised to 1.5 ms.

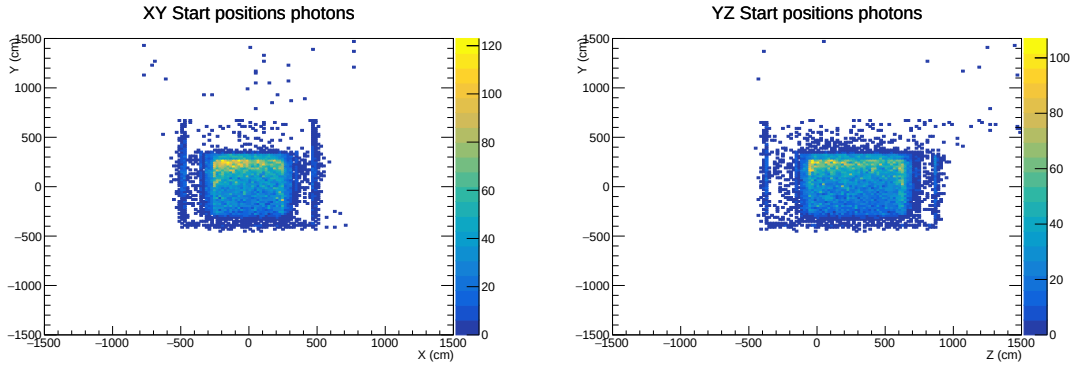

(a) (b)

Figure 7: Start position of photons which enter the active volume of the detector in the downstream view (a) and side view (b). The sample does not contain an overburden.

3.2 Cosmic induced background

Secondary photons and electrons impose a background to the sterile neutrino searches of the experiment. Their electromagnetic shower can mimic the signal of ν_e appearance or single photon searches. Electromagnetic showers are in most cases induced by primary muons producing a delta-electron that radiates a photon through bremsstrahlung, or a photon produced directly by the primary muon through bremsstrahlung. These are the primary sources of cosmogenic background. Other, non-negligible

Particle Type	Primaries	CORSIKA CMC FLUKA Secondaries	Total
μ^-	8.926 ± 0.021	0.0020 ± 0.0001	8.928 ± 0.021
μ^+	11.079 ± 0.024	0.0014 ± 0.0003	11.093 ± 0.024
neutron	0.036 ± 0.001	0.508 ± 0.005	0.544 ± 0.006
proton	0.0006 ± 0.0002	0.2458 ± 0.0035	0.246 ± 0.004
γ (>100 MeV)	0.0002 ± 0.00001	0.0032 ± 0.0004	0.0034 ± 0.0005
e^- (>100 MeV)	0.0 ± 0.0	0.0020 ± 0.0003	0.0020 ± 0.0003
e^+ (>100 MeV)	0.0 ± 0.0	0.0020 ± 0.0003	0.0020 ± 0.0003

Table 2: The particle rates expected in the detector with overburden, normalised to 1.5 ms.

processes are in more detail described in [4].

The reduction in Table 2 shows that an overburden of 1 m thickness does significantly decrease the number of neutrons and protons by 35 % and 52 %, respectively. As previous studies have shown, neutrons and protons represent the main source of non-muon and non-photon induced background showers [4].

The overburden does not have a significant effect on the number of muons in the TPC. Since primary muons are the largest contributor to the cosmogenic background, special attention has to be dedicated to the reduction of the muon-induced background.

Figures 8, 9, 10, 11 show the energies of all primary and secondary particles and those which enter the TPC without overburden. One can see that the majority of primary photons does not reach the detector. However, as mentioned above, secondary photons are generated in large numbers in the detector. In particular, also at low energies, corresponding to the signal region.

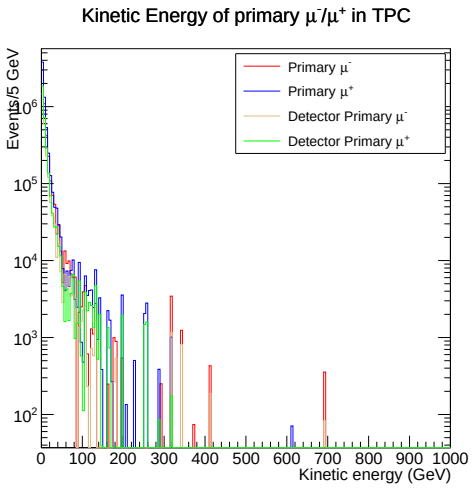

(a) Primary muons

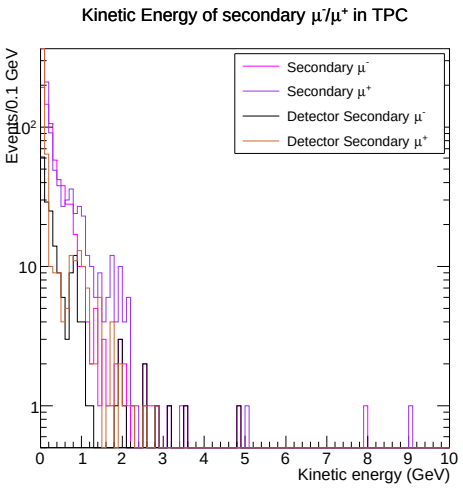

(b) Secondary muons

Figure 8

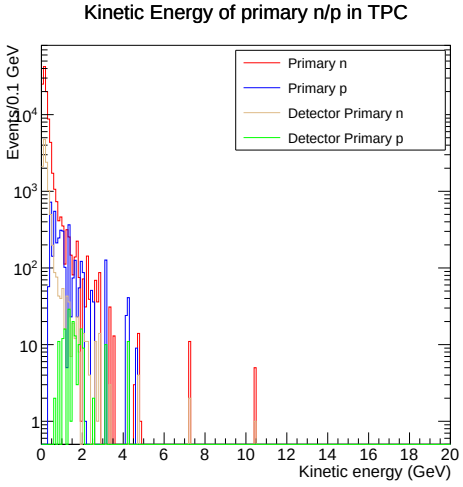

(a) Primary neutrons and protons

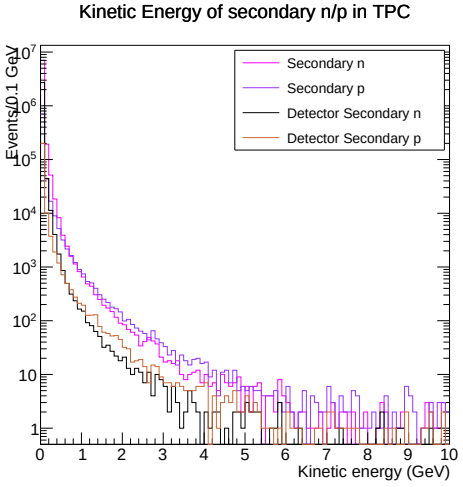

(b) Secondary neutrons and protons

Figure 9

4 Photon background reduction

To address secondary photons induced by muons a muon cylinder cut is introduced, as illustrated in Figure 12a. A cylinder is defined around a muon track. For this purpose, the muon track is assumed to be straight and the track is determined by

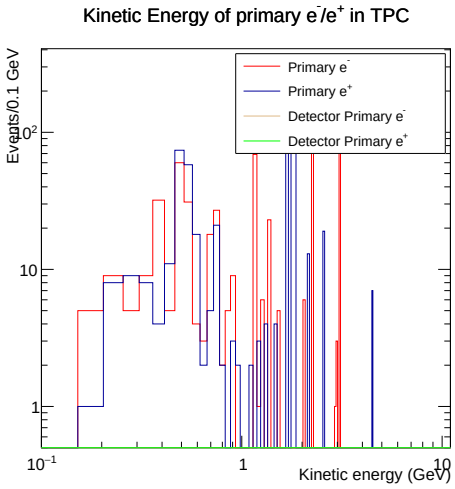

(a) Primary electrons

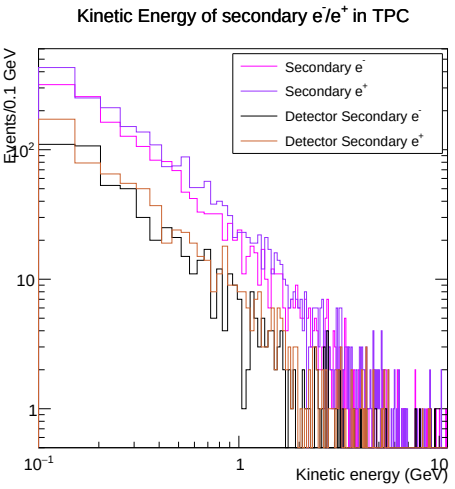

(b) Secondary electrons

Figure 10

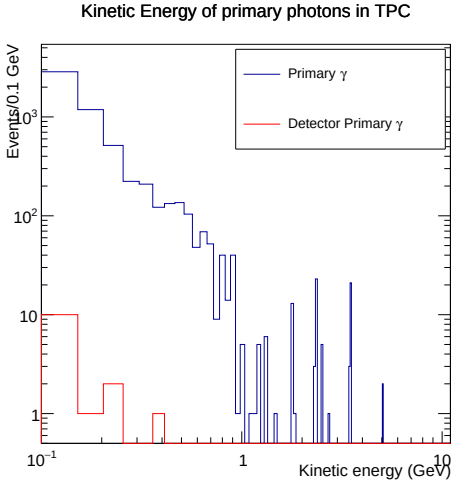

(a) Primary photons

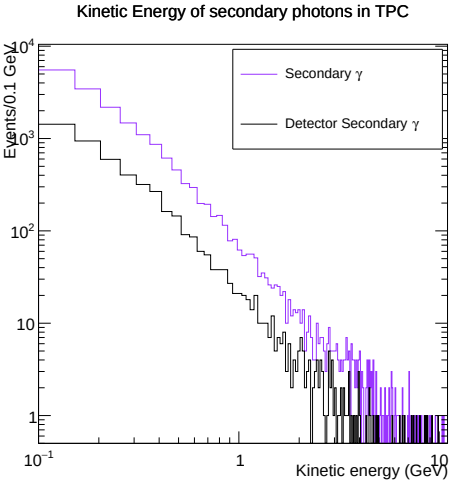

(b) Secondary photons

Figure 11

its start position and momentum. If a photon, which has the muon as its primary ancestor, converts inside the cylinder, it is rejected. This method assumes a 100 % muon detection efficiency of the cosmic ray detection planes and has to be adjusted accordingly once the muon detection efficiency has been determined. Figure 12b shows the distance that photons travel which originate from a primary muon. One

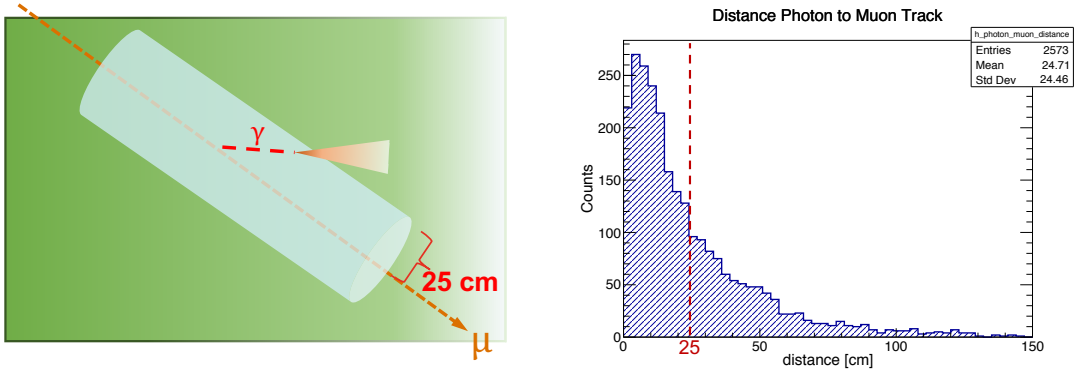

(a) (b)

Figure 12: Figure (a) illustrates the muon cylinder cut. A radial volume around a muon track is defined around which all photon induced showers are not taken into account. (b) shows the radial distance of photons to their ancestor muon track. A cylinder cut of 25 cm would significantly reduce the background.

can see that a cylinder with a radius of 25 cm would significantly reduce the number of background photons.

Further options to reduce the background include the definition of a fiducial volume or a backward-distance-to-wall (BDtoW) cut. The former describes a volume inside the TPC. All events outside this volume are rejected. This accounts for higher activities close to the walls of the cryostat. For the purpose of this study, the fiducial volume is defined with a distance of 25 cm to all walls of the TPC, except in beam direction. There, the distance to the upstream wall is set to 30 cm and to the downstream wall to 100 cm, as illustrated in Figure 13a, following the convention of the MicroBooNE collaboration [4].

The BDtoW cut considers the distance of a photon to the nearest wall in flight direction, as illustrated in Figure 13b. If this distance is below a certain threshold the event is rejected. This threshold is defined as 25 cm in this study.

The flight direction of the photon is determined by its momentum. It is important to note that this information is only available in the MC simulation and not in data. The reconstructed photon induced electromagnetic shower direction would serve the

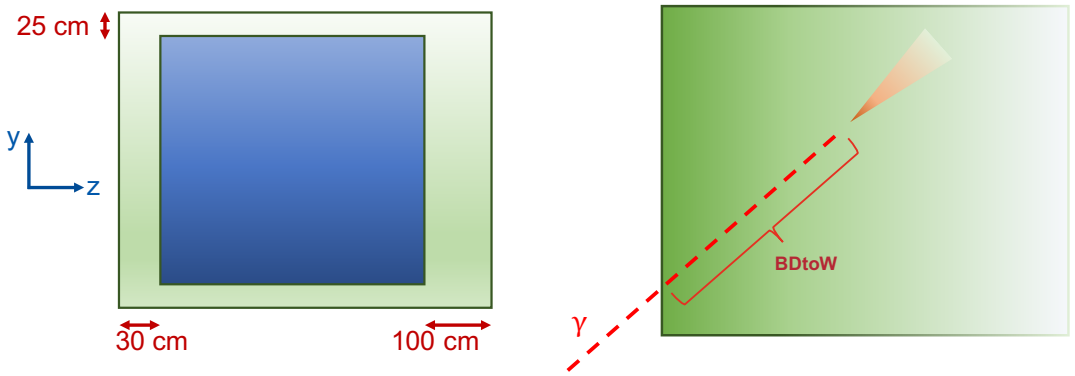

(a) (b)

Figure 13: Figure (a) illustrates the definition of the fiducial volume inside the TPC as 30 cm to the upstream wall, 100 cm to the downstream wall, and 25 cm to all other walls. Figure (b) shows the backward-distance-to-wall cut which rejects events based on the distance of a photon to the nearest TPC, measured in flight direction.

same purpose but is subject to reconstruction uncertainties, which could reduce the accuracy of this cut criterion.

Figure 14 shows the energy distribution of single photons inside the TPC. In red the total number of photons is shown. The blue curve indicates the energies of the photons which are denoted in this context as *untaggable*, meaning that they are outside the defined muon cylinder or they are invisible due to one of the following two reasons: all of the ancestors of the photon up to the one entering the TPC are neutral and hence do not leave a trace in the liquid argon, or the photon entering the TPC was generated outside the active volume. The fraction of untaggable photons which are not rejected by the BDtoW cut is coloured in brown, and the fraction of untaggable photons that are inside the fiducial volume in green. One can see that the fraction of photons which are denoted as untaggable are only 30 % of the total number of photons in the TPC. This number is further reduced by introducing the BDtoW cut (19 %) or alternatively the fiducial volume cut (10 %).

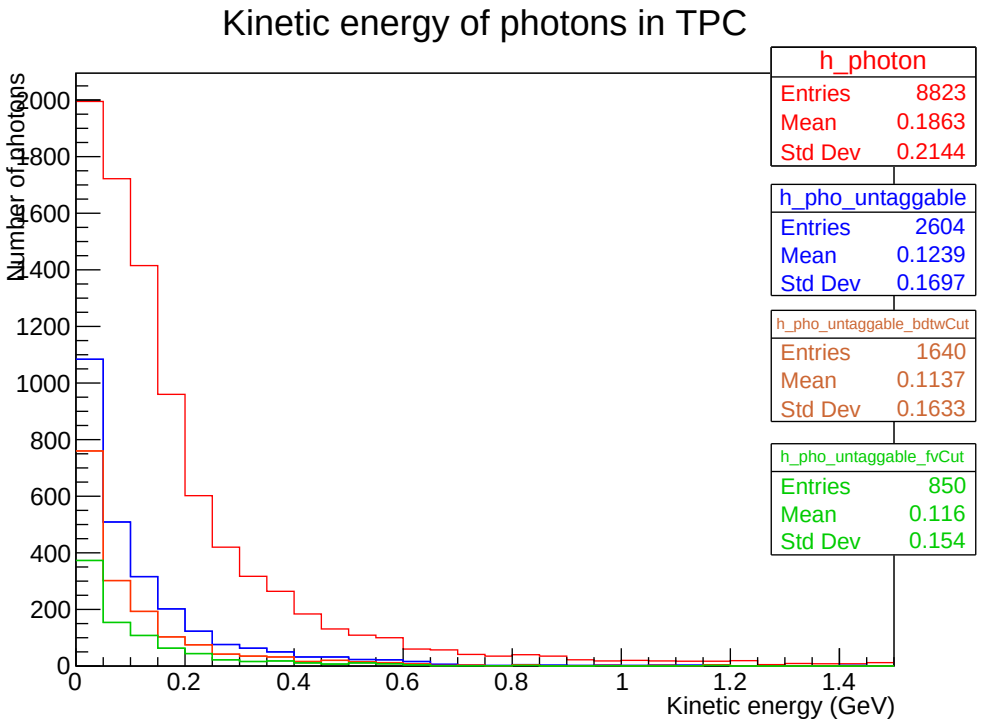

Figure 14: The photon background reduction due to several cuts is shown. The red curve represents the total number of photons in the TPC. Untaggable photons are shown by the blue curve. The untaggable photons which are not rejected by the BDtoW cut are represented by the brown curve and the untaggable photons which are inside the fiducial volume are represented by the green curve.

5 Conclusion

The study has successfully validated the detector geometry simulation and cosmic particle generation. A comparison of the expected particle rates for the cases of no overburden and an overburden of 1 m thickness was made. As expected, the number of muons is not affected to a large extent by the overburden. The number of protons and neutrons which are the largest source of non-muon and non-photon induced background is significantly reduced by the overburden. For a more effective shielding from cosmic particles, an increase in thickness of the overburden is suggested, as well as an increased area in the horizontal plane to absorb cosmic particles with a larger angle of inclination. Special attention has to dedicated to the downstream region

of the detector which is subject to a larger cosmogenic backround rate due to the building structure.
The number of photons in the TPC was largely reduced by the muon cylinder cut, the BDtoW cut, and the fiducial volume cut. The remaining number of muons would, however, still significantly affect the search for ν_e appearance. Hence, further cuts have to be introduced or the existing cuts refined in order to reach an optimal background reduction efficiency with low signal rejection.

References

[1] R Acciarri, C Adams, R An, C Andreopoulos, AM Ankowski, M Antonello, J Asaadi, W Badgett, L Bagby, B Baibussinov, et al. A proposal for a three detector short-baseline neutrino oscillation program in the fermilab booster neutrino beam. *arXiv preprint arXiv:1503.01520*, 2015.

[2] Sea Agostinelli, John Allison, K al Amako, J Apostolakis, H Araujo, P Arce, M Asai, D Axen, S Banerjee, G Barrand, et al. Geant4—a simulation toolkit. *Nuclear instruments and methods in physics research section A: Accelerators, Spectrometers, Detectors and Associated Equipment*, 506(3):250–303, 2003.

[3] Radovan Chytracek, Jeremy McCormick, Witold Pokorski, and Giovanni Santin. Geometry description markup language for physics simulation and analysis applications. *IEEE Transactions on Nuclear Science*, 53(5):2892–2896, 2006.

[4] MicroBooNE Collaboration et al. Cosmic shielding studies at microboone. Technical report, MICROBOONE-NOTE-1005-PUB, 2016. URL http://www-microboone. fnal. gov/publications/publicnotes/index. html, 2016.

[5] Chris Hagmann, David Lange, and Douglas Wright. Cosmic-ray shower generator (cry) for monte carlo transport codes. In *Nuclear Science Symposium Conference Record, 2007. NSS'07. IEEE*, volume 2, pages 1143–1146. IEEE, 2007.

[6] Dieter Heck, Tanguy Pierog, and Johannes Knapp. Corsika: An air shower simulation program. *Astrophysics Source Code Library*, 2012.

[7] Fermi National Accelerator Laboratory. https://fnal.gov, 2017. accessed 18 Sept 2017.